REPORT DOCUMENTATION PAGE

Form Approved
OMB No. 0704-0188

1. REPORT DATE *(DD-MM-YYYY)*	**2. REPORT TYPE**	**3. DATES COVERED** *(From - To)*
2012	Open Literature	

4. TITLE AND SUBTITLE
Pathogenesis of acute and delayed corneal lesions after ocular exposure to sulfur mustard vapor

5a. CONTRACT NUMBER

5b. GRANT NUMBER

5c. PROGRAM ELEMENT NUMBER

6. AUTHOR(S)
McNutt, P, Hamilton, T, Nelson, M, Adkins, A, Swartz, A, Lawrence, R, Milhorn, D

5d. PROJECT NUMBER

5e. TASK NUMBER

5f. WORK UNIT NUMBER

7. PERFORMING ORGANIZATION NAME(S) AND ADDRESS(ES)

US Army Medical Research Institute of Chemical Defense
ATTN: MCMR-CDR-C
3100 Ricketts Point Road
Aberdeen Proving Ground, MD
21010-5400

8. PERFORMING ORGANIZATION REPORT NUMBER

USAMRICD-P11-006

9. SPONSORING / MONITORING AGENCY NAME(S) AND ADDRESS(ES)
Defense Threat Reduction Agency
8725 John J. Kingman Road STOP 6201
Fort Belvoir, VA 22060-6201

10. SPONSOR/MONITOR'S ACRONYM(S)

11. SPONSOR/MONITOR'S REPORT NUMBER(S)

12. DISTRIBUTION / AVAILABILITY STATEMENT

Approved for public release; distribution unlimited

13. SUPPLEMENTARY NOTES
Published in Cornea, 31(3), 280-290, 2012. This research was supported by the Defense Threat Reduction Agency- Joint Science and Technology Office, Medical S&T Division (grant numbers 2.F0012_07_RC_C, CBM.CUTOC.01.RC.003).

14. ABSTRACT
See reprint.

15. SUBJECT TERMS
mustard gas keratopathy, ocular toxicity, vapor exposure, sulfur mustard, chemical warfare agent, medical chemical defense

16. SECURITY CLASSIFICATION OF:			**17. LIMITATION OF ABSTRACT**	**18. NUMBER OF PAGES**	**19a. NAME OF RESPONSIBLE PERSON**
a. REPORT	**b. ABSTRACT**	**c. THIS PAGE**			Patrick McNutt
UNCLASSIFIED	UNCLASSIFIED	UNCLASSIFIED	UNLIMITED	11	**19b. TELEPHONE NUMBER** *(include area code)* 410-436-8044

Pathogenesis of Acute and Delayed Corneal Lesions After Ocular Exposure to Sulfur Mustard Vapor

Patrick McNutt, PhD, Tracey Hamilton, BS,* Marian Nelson, BS,* Angela Adkins, BA,* Adam Swartz, MS,* Richard Lawrence, BS,* and Denise Milhorn, PhD†*

Purpose: Sulfur mustard (SM) exposure results in dose-dependent morbidities caused by cytotoxicity and vesication. Although lesions resulting from ocular exposure often resolve clinically, an idiopathic delayed mustard gas keratopathy (MGK) can develop after a moderate or severe exposure. Sequelae include persistent keratitis, recurring epithelial lesions, corneal neovascularization, and corneal degeneration, which can lead to impaired vision or loss of sight. The purpose of this effort is to correlate structural changes with injury progression during the development of MGK.

Methods: New Zealand White rabbit corneas were exposed to SM using a vapor cup delivery system. The transition from acute to delayed injury was characterized by clinical, histological, and ultrastructural metrics over 8 weeks.

Results: Exposure dose was correlated to the likelihood of developing MGK but not to its severity. In a 56-animal cohort, a 2.5-minute exposure generated a corneal lesion, with 89% of corneas developing MGK within 5 weeks. A significant decrease in corneal edema at 2 weeks was predictive of the 11% of corneas that underwent asymptomatic recovery. Ultrastructural comparison of asymptomatic and MGK corneas at 8 weeks indicates that MGK is characterized by persistent edema and profound disorganization of the basement membrane zone.

Conclusions: Ultrastructural changes associated with the delayed pathophysiology of corneal SM vapor exposure involve severe degeneration of the basement membrane zone and persistent edema. The mechanisms underlying MGK pathogenesis seem to alter injury progression as soon as 2 weeks after exposure. These data suggest that the vapor cup model system is suitable for therapeutic evaluation.

Key Words: mustard gas keratopathy, ocular toxicity, vapor exposure, sulfur mustard

(*Cornea* 2012;31:280–290)

Sulfur mustard (2,2′-dichloroethylsulfide; SM) is a highly reactive bifunctional chemical that alkylates proteins and nucleic acids. Battlefield deployment of SM as a chemical weapon in World War I and the Iran–Iraq war resulted in more than 210,000 British and Iranian casualties, 90% of which presented with ocular lesions.[1] In humans, the acute stage of ocular SM toxicity involves dose-dependent morbidities caused by vesication of the corneal epithelium (CE) and keratocytosis in the epithelium and stroma. Eyes are the most sensitive organ to SM injury, and although mild exposures typically resolve uneventfully, those that receive moderate or severe exposures (exceeding 100 $\mu g \cdot min^{-1} \cdot m^{-3}$) exhibit 3 distinct clinical trajectories: (1) injury resolution, after which the victim remains asymptomatic; (2) persistent keratitis that ultimately results in corneal degeneration (chronic injury); or (iii) an asymptomatic period followed by reemergence of lesions (delayed-onset injury).[1,2] The latter 2 trajectories comprise the phenomenon known as mustard gas keratopathy (MGK), which has been diagnosed in 16% of casualties receiving a moderate or worse exposure.[3,4]

MGK is characterized by a persistent inflammatory condition in the cornea (keratitis) followed by development of secondary keratopathies, such as recurring corneal epithelial erosions (RCEs) and neovascularization (NV). In the chronic form of SM toxicity, MGK symptoms develop from the acute injury; alternatively, the delayed-onset form appears after an asymptomatic latent period lasting 0.5 to 40 years.[5] Histology of corneas excised from MGK patients undergoing penetrating keratoplasty displays sequelae of chronic inflammation, such as stromal degeneration and necrosis, suggesting a persistent injury that is beyond the healing capacity of the cornea.[2,6,7] Similar findings were reported after in vivo confocal microscopy of SM survivors with moderate symptoms of MGK.[8]

Received for publication June 23, 2011; revision received August 19, 2011; accepted August 24, 2011.

From the *United States Army Medical Research Institute of Chemical Defense, Gunpowder, MD; and †United States Army Medical Research and Materiel Command, Fort Detrick, MD.

Supported by the Defense Threat Reduction Agency—Joint Science and Technology Office, Medical S&T Division (grant numbers 2. F0012_07_RC_C, CBM.CUTOC.01.10.RC.003).

The authors state that they have no financial or conflicts of interest to disclose.

The views expressed in this article are those of the authors and do not reflect the official policy of the Department of Army, Department of Defense, or the US Government. The experimental protocol was approved by the Animal Care and Use Committee at the United States Army Medical Research Institute of Chemical Defense, and all procedures were conducted in accordance with the principles stated in the Guide for the Care and Use of Laboratory Animals (National Research Council, 1996), and the Animal Welfare Act of 1966 (P.L. 89-544), as amended.

Supplemental digital content is available for this article. Direct URL citations appear in the printed text and are provided in the HTML and PDF versions of this article on the journal's Web site (www.corneajrnl.com).

Reprints: Patrick McNutt, United States Army Medical Research Institute of Chemical Defense, 3100 Ricketts Point Rd, Gunpowder, MD 21010 (e-mail: patrick.mcnutt@us.army.mil).

The standard of care for acute SM lesions is similar to that of other corneal abrasions (eg, irrigation, topical mydriatics, antibiotics, and steroids); however, in animal models, these do not seem to attenuate late ocular complications.[1,9] Because the etiologies of the MGK sequelae are unknown, therapeutic strategies have predominantly been supportive and applied succedent to the onset of symptoms.[10,11] In the more severe cases, penetrating keratoplasty has been attempted with mixed outcomes.[2,6] Given the threat of permanent visual impairment and chronic discomfort among victims of ocular SM injury, there is a critical need for an effective therapeutic that mitigates long-term toxicity.

Rabbits have been a model system for ocular SM injury for more than 60 years.[12,13] They exhibit several anatomical and physiological features that facilitate ocular toxicology research, such as a large corneal to sclera ratio, a relative insensitivity to corneal drying, and a low frequency of spontaneous epithelial lesions.[14] Rabbit corneas have greater structural similarity to human eyes than do mice, rat, or guinea pig corneas, and although rabbits are 4-fold less sensitive to ocular SM injury than humans, at normalized doses, they display similar sequelae and injury progression.[12,15] Recently, rabbit exposure models have been used to evaluate candidate treatments, test novel ocular delivery systems, and evaluate long-term SM toxicology in the limbus.[9,16–18]

The traditional model of corneal exposure uses liquid drops of SM applied directly to the cornea.[12] This generates a localized ulcerative injury as opposed to the milder, more evenly distributed injury incurred by vapor exposure.[13] Nonetheless, researchers have historically used liquid SM out of concerns that mechanical injury incurred by the cornea during vapor cup delivery might compromise ultrastructural and toxicological evaluation. Although goggle-based delivery of SM vapor to the entire eye avoids these concerns and more closely reflects a battlefield injury, the specific progression of corneal injury and contribution of corneal injury to MGK is complicated by injury to the ocular adnexa, which may influence the extent or degree of corneal pathogenesis.[19] Thus, although corneal complications are the signature of moderate and severe long-term ocular SM injury, the keratopathogenesis of long-term toxicities after a diffuse exposure has not been well described.[11] We previously reported on a vapor cup system to deliver SM vapor to the cornea of New Zealand White rabbits.[20] In preliminary work, we demonstrated that exposure of rabbit corneas to SM vapor resulted in vesicating injuries and at higher doses caused recurring lesions.[20] This exposure model was not observed to cause direct SM injury to noncorneal tissues, allowing an emphasis on mechanisms of corneal pathogenesis. In this report, we use the vapor cup model to characterize clinical and histological characteristics of the transition from the acute injury to the delayed injury and for the first time present ultrastructural changes associated with the pathophysiology of corneal SM vapor exposure.

MATERIALS AND METHODS

Animal Use

Rabbit experiments involved 3 cohorts. In the first cohort, 30 corneas were exposed to SM vapor for 1 to 3.5 minutes (n = 5 per dose), followed by weekly evaluations and histopathological analysis at 6 weeks. The second involved exposure of 28 animals for 2.5 minutes followed by histopathological characterization at 1 to 7 days. The third involved exposure of 56 animals for 2.5 minutes followed by regular clinical evaluations and histology/transmission electron microscopy (TEM) at 8 weeks.

Rabbits were ordered from Charles River Laboratories at 2 to 2.5 kg and caged individually on an enriched diet ad libitum. Before exposure, animals underwent a baseline corneal evaluation. On the day of exposure, a surgical plane was induced by intramuscular injection of ketamine HCl (15 mg/kg) and xylazine (7 mg/kg), and a loading dose of buprenorphine HCl (0.05 mg/mL) was administered subcutaneously. Osmotic pumps (Alzet, Cupertino, CA) primed to deliver 10 μL/h of buprenorphine HCl (0.3 mg/mL) for 7 days were implanted subdermally between the scapulae. After exposure, animals were returned to individual cages and monitored daily. Pumps were removed 7 days after implantation. At the termination of each experiment, animals were euthanized by cardiac delivery of 2 mL of pentobarbital sodium (390 mg/mL).

Exposure Procedures

Before exposure, 10 μL of neat SM was distributed on Whatman filter paper firmly lodged in the bottom of a 14 × 5.2-mm deep screw cap modified with a 12-mm rubber O-ring, designed to minimize mechanical injury to the cornea and to form a capillary seal with the tear film. Loaded caps were inverted for 1 minute and placed directly over the center of the rabbit eye for 1 to 4 minutes. After exposure, animals were monitored for 2 minutes, and remaining agent was gently flushed from the eye with 10 mL of sterile saline. The contralateral eye served as an exposure control. No adverse outcomes were observed in control eyes with saline-soaked vapor cups. Exposure hoods were maintained at 22 to 22.5°C and at 35% to 45% humidity.

Clinical Evaluations

Rabbits were evaluated at regular intervals starting 24 hours after exposure. The presence of corneal epithelial lesions was characterized by blue light photography of eyes 1 minute after treatment with 40 μL of fluorescein; retained fluorescein is indicated of a disruption in epithelial integrity. Planimetric lesion size was calculated on photographs using NIH Image after image registration. Pachymetry and slit-lamp examination were used to quantify corneal edema, and white light evaluation was used to identify opacity and NV. Corneal epithelial erosions and NV were graded as present or absent. Changes in mean corneal thickness and planimetric lesion size were compared using a *t* test.

Histopathology and TEM

After enucleation, eyes were fixed by injection of buffered 1.6% paraformaldehyde and 2.5% glutaraldehyde into the posterior chamber, followed by immersion in the same at 4°C for 24 to 28 hours. Corneas were excised and

representative areas of tissue to include any gross lesions were isolated by scalpel and processed for routine histopathology and TEM. Light microscopy was performed using an Olympus BX51 microscope. Categorical scoring for histopathology used the following system: "0" = no evidence of injury, "1" = injury is present over <10% of the area, "2" = injury over 11% to 25% of area, "3" = injury over 26% to 50% of area, and "4" = injury over 51% to 100% of area. The degree and extent of epithelial and stromal sequelae were graded similar to Milhorn et al[20] to include ulceration, edema, necrosis, deformation, NV, and inflammation, and scores were summed, then compared by the Mann–Whitney rank sum test with Bonferroni adjustment. The mean number of heterophils in 2 hematoxylin and eosin–stained sagittal sections per cornea were averaged across 4 cornea per time point and compared using a *t* test.

Tissues selected for TEM were postfixed in buffered 1% osmium tetroxide, dehydrated in graded ethanol, and embedded in Poly/Bed 812 resin. Semithin sections (1.5 μm thick) were stained in 1% methylene blue and 1% azure II. Ultrathin sections (90 nm thick) were mounted on copper mesh grids and counterstained using uranyl acetate and lead citrate. The observation of sequelae in micrographs from at least 3 corneas were considered to be genuine. TEM was performed using a JEOL JEM-1230 transmission electron microscope.

Gas Chromatography–Mass Spectrometry

Rabbit plasma was collected and clarified by centrifugation at 2000*g* for 30 minutes at 5°C. Protein from plasma samples obtained from exposed animals or spiked standards was isolated and prepared as described with the following modifications.[21] Plasma protein was extracted from 1 mL of plasma by 3 washes with acetone, and precipitated protein was dried. The protein pellet was weighed and digested at 125 mg/mL in 1M NaOH at 70°C. Digested protein was doped with 0.6 ng of the internal standard octadeuterothiodiglycol, pH adjusted with 3M HCl, and extracted with neat ethyl acetate. Extracts were derivatized, passed over preconditioned Bond Elute silica 100-mg Si SPE cartridges and evaluated by gas chromatography–mass spectrometry. Calibration curves were prepared using rabbit plasma treated with 0.78 to 50 nM SM for 2 hours at 37°C. Protein precipitated from the calibration curve samples was processed as described above. Calibration curves established a limit of detection of 0.07 ng/mL and a limit of quantitation of 0.24 ng/mL and were used with each set of rabbit samples to calculate plasma SM concentrations. Sample means were compared across dose and time by *t* test.

RESULTS

Acute and Delayed SM Toxicity Is Dose Dependent

To correlate exposure dose with long-term outcomes, we used the vapor cup model to deliver SM vapor to rabbit corneas for 1 to 3.5 minutes, evaluated the clinical status at weekly intervals, then scored the corneal histopathology at 6 weeks. All animals underwent an acute injury characterized by corneal edema, corneal opacity, and epithelial lesions (Fig. 1A, top panels). After partial healing of the acute injury, a second set of pathologies developed between 3 and 5 weeks, in which corneas exhibited increased corneal edema, immune cell infiltrates, RCEs, and NV (Fig. 1A, bottom panels). Clinical evaluations indicated a strong relationship between dose and the

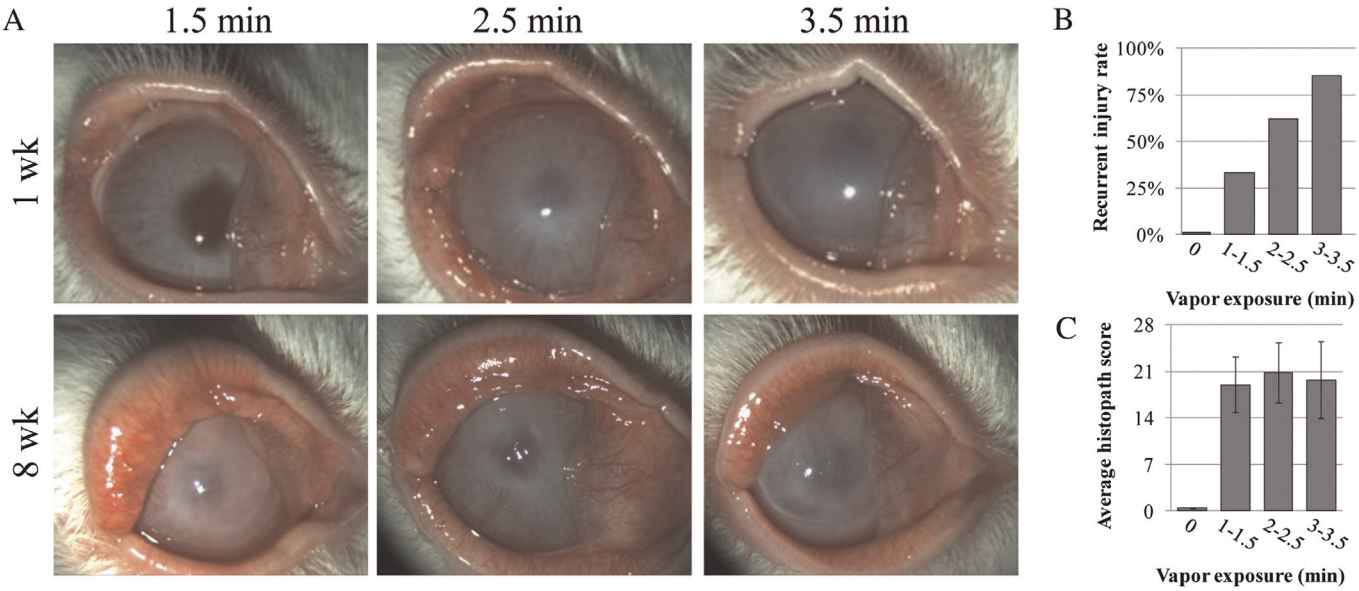

FIGURE 1. Severity of acute injury and frequency of delayed symptoms correlate well with dose, whereas severity of delayed injury does not. A, Corneas demonstrated escalating severity of acute sequelae at 1 week but similar severity in delayed-onset injury at 8 weeks. B, Frequency of development of late-onset symptoms at different durations of SM vapors exposure. C, Cumulative histopathology scores at different doses.

likelihood of developing delayed keratopathies (Fig. 1B), but histopathology suggested that the dose was not related to the severity of delayed keratopathies (Fig. 1C). Based on these data, we selected a 2.5-minute exposure for future work because this produced corneal injuries similar to those resulting from moderate-to-severe SM exposures in humans, with a high prevalence of recurring lesions for therapeutic testing.[11]

The Acute Lesion Involves Vesication of the CE and Corneal Cytotoxicity

All exposed corneas developed an epithelial lesion within 1 day (Fig. 2A). Although lesion morphology changed between 1 and 2 days, the total lesion area did not, suggesting competing processes of in-migration and lesion expansion (Fig. 2B). The CE regenerated and became refractory to the fluorescein assay in 96% of corneas by 4 days (a photographic panel of reepithelialization is presented in Supplemental Digital Content 1, http://links.lww.com/ICO/A32). Stromal edema was present immediately under the denuded cornea as soon as 1 day after exposure (Figs. 2C, D).[20]

Ultrastructural changes associated with acute toxicity were evaluated by TEM (Fig. 3). As is typical with vesicating injuries, separation between the epithelium and stroma occurred within the lamina lucida (Fig. 3B).[22] Migrating epithelial cells could be observed as soon as 2 days. Desmosomal attachments between epithelial cells suggest that migration occurred as an epithelial sheet (Fig. 3C), and the basal membranes were highly involuted, indicative of a mobile population forming transient adhesions to the basement membrane (Fig. 3D). By 4 days, nascent hemidesmosomal densities in the basal membranes of CE cells and associated anchoring plaques in the Bowman-like layer (BLL) became apparent (Figs. 3E, F). By 7 days, the CE was stratified with maturing basement membrane zone (BMZ) architecture (Fig. 3F). Conversely, the stroma continued to show signs of edema and immune cell infiltration, with necrotic fibrocytes distributed through the stromal volume underlying the exposure site appearing as soon as 1 day after SM treatment (Figs. 3H, I).

Delayed Injury Frequencies Within Experimental Cohorts Suggest That Multiple Clinical Outcomes Are Possible

To evaluate the development of MGK from the acute injury, 56 corneas were longitudinally evaluated using clinical metrics over 8 weeks. Despite regeneration of an intact epithelium within 5 days (which also is the point of maximum edema during the acute injury), 89% continued to exhibit a persistent keratitis characterized by elevated edema (Fig. 4A) and immune cell infiltrates (Fig. 4B). Of these, 80% subsequently developed secondary keratopathies between 3 and 5 weeks with RCEs (Figs. 4C, D) and NV (Fig. 4C). Interestingly, although recurring lesions were only about one third to one half the size of the acute lesions, the morphology varied on a weekly basis, suggesting cyclic attempts to reepithelialize followed by the development of new lesions (Fig. 5, bottom panels, days 21–56). The remaining 11% of animals progressively became asymptomatic, with healthy appearing corneas and minimal opacity by 2 weeks, a decline in corneal thickness to baseline values by 5 weeks, and failure to develop RCEs or NV. Notably, corneas undergoing asymptomatic recovery could be distinguished as soon as 2 weeks after exposure by a significant decrease in corneal thickness (Fig. 4E, dashed line). Despite persistent markers of inflammation in all corneas that would develop MGK, there was only mild evidence of corneal injury until secondary keratopathies developed (Fig. 5, days 7–21). No cornea that transitioned to a persistent keratitis subsequently exhibited clinical improvement or resolution within 8 weeks. A summary of clinical outcomes and characteristic sequelae is presented in Table 1.

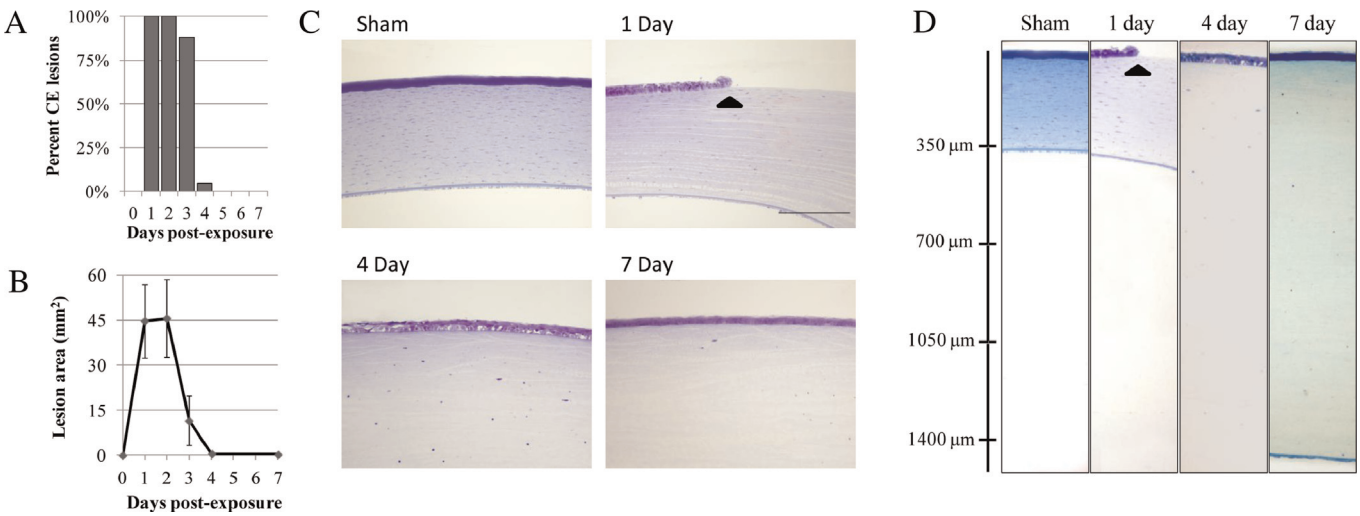

FIGURE 2. Clinical and histopathological metrics of the acute injury. A, Planimetric area of fluorescein staining in exposed and sham-exposed corneas (n = 25). B, Percent of corneas exhibiting fluorescein retention over the first week after exposure (n = 75). C, Thin sections demonstrating histological changes during the acute injury (×4). Scale bar = 200 μm. D, Full corneal strips (×10) from same slides in (C). At 4 days, it was not possible to image the entire stroma due to the extent of edema. Arrowheads represent margin of acute lesion.

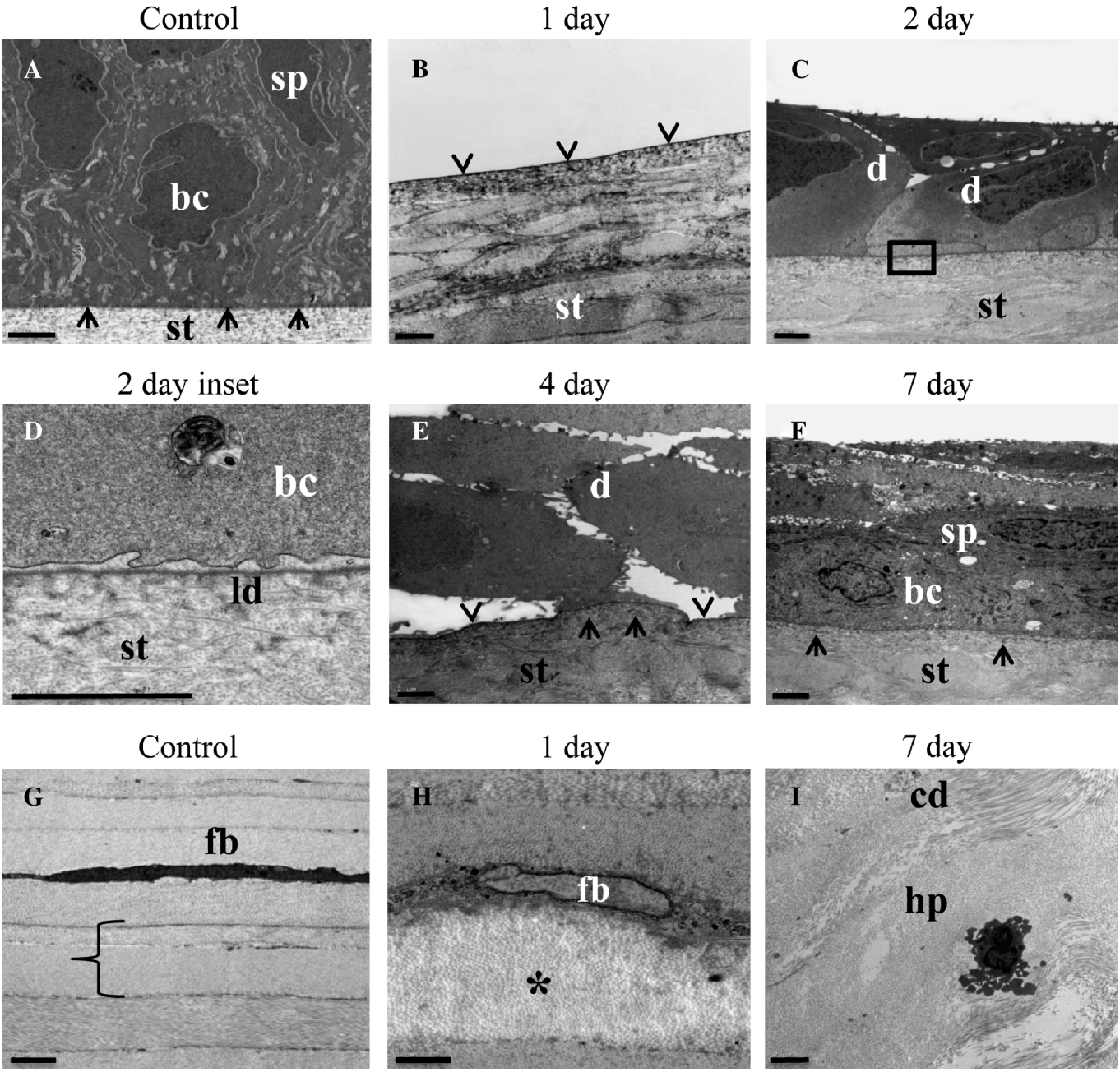

FIGURE 3. Representative electron micrograph images of the BMZ and stroma over 1 week after SM vapor exposure. A and G, Electron micrographs of sham-exposed BMZ and stroma. B, C, E, and F, Injury progression in the BMZ at 1, 2, 4, and 7 days, respectively. H and I, Injury progression in the stroma at days 1 and 7. bc, basal epithelial cell; cd, cellular debris; d, desmosomal attachments; fb, fibrocyte; hp, infiltrating heterophils; ld, lamina densa; sp, suprabasal cell; and st, stroma. Brackets indicate lamellae, arrowheads indicate lamina densa, and arrows indicate hemidesmosomal attachments. All scale bars are 2 μm.

Resolved Corneas Do Not Exhibit the Severe Ultrastructural Disorganization Displayed in Corneas Experiencing Late SM Lesions

In resolved corneas 8 weeks after exposure (Fig. 6A; also see Supplemental Digital Content 2, http://links.lww.com/ICO/A33, for clinical metrics and gross images), the CE was fully stratified and of normal thickness, with extensive desmosomes and without evidence of intercellular edema (Fig. 6B). Although the BMZ was not yet fully mature, there were numerous hemidesmosomal densities and associated anchoring plaques in the BLL, and the lamina lucida and lamina densa were well developed without disruption (Fig. 6C). Although necrotic remnants of basal epithelial cell intrusion into the stroma were occasionally observed, they were

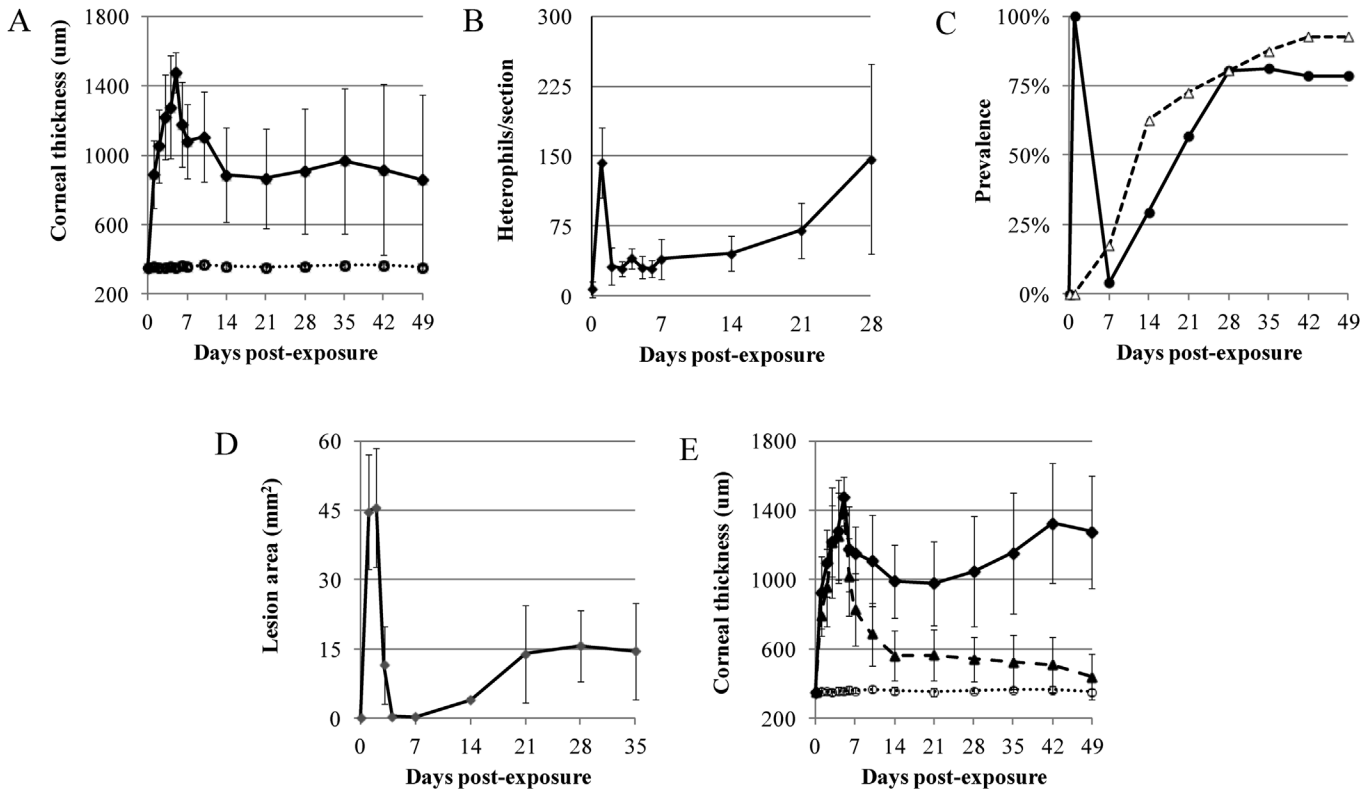

FIGURE 4. Longitudinal changes in metrics of delayed injury. A, Corneal thickness in injured (solid line) versus sham (dashed line) animals (n > 56; $P < 0.01$ at all time points compared with sham animals). B, Enumeration of heterophil infiltrates (n = 4 per time point; $P < 0.01$ between 1 day and 2–21 days). C, Incidence of RCEs (solid line) and NV (dashed line). N > 56 at all time points. D, Planimetric area of fluorescein retention (n = 25). Sham exposures resulted in no fluorescein retention. E, Comparison of corneal thicknesses of resolved corneas (solid line; n = 6) versus nonresolved corneas (dashed line; n = 50) and sham-exposed corneas (dotted line; n = 10). Statistical significances: $P < 0.01$ between MGK and sham corneas at all time points; $P < 0.05$ between resolved and MGK corneas at 2 weeks and beyond; resolved and sham corneas become indistinguishable at 5 weeks and beyond.

structurally isolated from the epithelium by a regenerated intact BMZ. The stroma exhibited a low-grade edema, with mild disruption of the lamellar structure and occasional infiltration of inflammatory cells (Fig. 6D).

Conversely, MGK corneas at 8 weeks exhibited severe ultrastructural degeneration consistent with the clinical and histological sequelae (Fig. 6E; also see Supplemental Digital Content 2, http://links.lww.com/ICO/A33, for clinical metrics and gross images), including extensive disruption of the BMZ, necrotic and apoptotic CE cells, incomplete and disorganized stratification of the CE, and significant stromal edema (Figs. 6E–H). In general, the BMZ was highly disorganized. The presence of redundant basal lamina was common, and numerous examples of basal cell processes extending through interruptions in the basement membrane into the BLL were observed (Figs. 6F, G). Basal epithelial cells exhibited an irregular distribution of hemidesmosomal densities ranging from rudimentary to complex in nature (Fig. 6G). Moderate to severe edema was present within the basal and suprabasal epithelial cell layers. Apoptotic bodies and cellular debris were also observed within extracellular gaps. Necrotic basal cells overlay the fragmented basement membrane, whereas desmosome-rich wing and superficial cell layers remained intact. The stroma was characterized by full-thickness edema, disorganized collagen fibrils, distorted lamella, heterophil infiltrates, and necrotic fibrocytes (Fig. 6H).

Differences in Clinical Outcome Cannot be Attributed to Variable Dosing

The observation that similar exposures resulted in significantly different outcomes raised the concern that corneas were receiving variable doses of SM vapor. Because SM-alkylated proteins can be identified in the plasma after cutaneous and inhalational exposures in a dose-dependent manner, we evaluated whether plasma adducts could be detected after ocular exposures.[21,23] Plasma adduct concentrations were tightly correlated with duration of exposure (dose; Fig. 7A; $R^2 > 0.98$) and cleared with a half-life of 130 ± 21 hours (Fig. 7B; $R^2 > 0.98$), similar to the half-life of rabbit albumin.[24,25] Applying this analysis to plasma isolated from the 56-animal cohort revealed a coefficient of variation of 31%, indicating a consistent exposure (Fig. 7C). Retrospective correlation of plasma adduct concentrations with clinical outcomes demonstrated no significant relationships with corneal thickness at 1 week (Fig. 7D; $R^2 < 0.01$), incidence of RCEs at 4 weeks, incidence of NV at 6 weeks (Fig. 7E), or animal weight at time of exposure (Fig. 7F; $R^2 < 0.12$). The

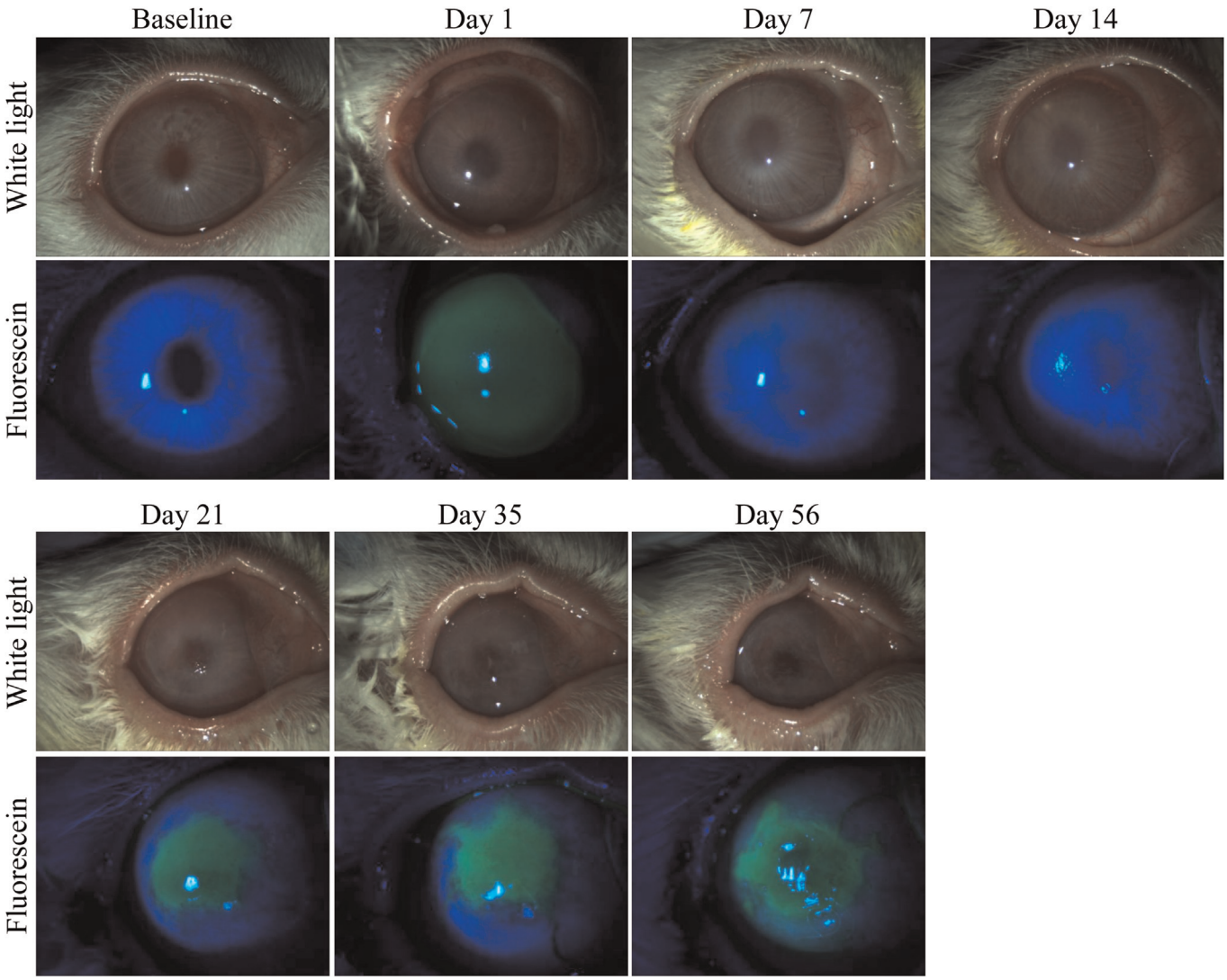

FIGURE 5. Longitudinal characterization of injury progression in a representative cornea over 8 weeks. White light photographs (×6.3, top panels) and images from fluorescein exclusion assay (×10, bottom panels) visualizing the acute injury and development of MGK in a characteristic rabbit.

slight correlation between adduct levels and animal weight is consistent with the change in plasma volume with respect to animal weight and therefore could reflect dilution in a larger plasma volume.[26] In some cases, animals receiving relatively large doses of SM exhibited no symptoms of MGK and vice versa. These data support the observation that factors other than dose can influence whether late SM lesions will develop and are likely to underlay the observation of diverse clinical outcomes within exposure cohorts.

DISCUSSION

Human and Rabbit Injury Progression After Corneal SM Exposure

In humans suffering from MGK, chronic inflammation results in corneal degeneration, permanently reducing visual acuity and potentially causing complete loss of vision.[5] The etiology of late SM lesions has been described as the product of a complicated series of processes, starting with direct SM injury to epithelial, stromal, and possibly endothelial tissues and leading to secondary responses in multiple cell types converging on the damaged cornea.[22] Multiple mechanisms of MGK have been proposed, including limbal stem cell deficiency, collagenase-resistant stromal–SM adducts inducing proinflammatory responses, basement membrane dystrophy, and barrier dysfunction resulting in persistent edema.[17,20,27] No therapeutic approach has succeeded in preventing late SM toxicity.

Our data suggest that vapor cup delivery to rabbit corneas produces a milder and more diffuse injury than liquid SM drops, providing increased consistency in ocular response with greater similarity to the characteristic human casualty.[12,13,28] Sham-exposed eyes exhibited neither clinical nor histopathological morbidities, and clinical outcomes were

TABLE 1. Summary of Clinical Outcomes Observed Within 8 Weeks of Ocular Vapor SM Exposure

Outcome	n (%)	Common Symptoms/ Sequelae
Acute injury	56/56 (100)	Edema, epithelial lesion, corneal cytosis
Long-term outcomes		
Injury resolution	6/56 (11)	Return to baseline values
Chronic injury	50/56 (89)	Persistent edema, immune cell infiltration
Secondary keratopathies	45/50 (90)	Recurring corneal erosions increased edema and immune cell infiltrates, increased opacity, NV, epithelial bullae, corneal degeneration
Persistent keratitis	5/50 (10)	No evidence of secondary keratopathies

similar to those reported for goggle-based vapor delivery models, suggesting that the vapor cup exposure model does not induce a mechanical injury to the cornea.[17] After a 2.5-minute vapor cup exposure, 89% of corneas transition to a persistent keratitis, with 80% subsequently developing symptoms similar to human MGK (RCEs, persistent edema, corneal degeneration, and inflammatory infiltrates) between 2 to 5 weeks after exposure. Although the eye appears grossly quiet during the period between acute injury and the development of secondary keratopathies, the injury is not clinically asymptomatic. There was no significant improvement in clinical or histological metrics of corneal health after the onset of delayed SM lesions, suggesting that this persistent keratitis is the rabbit equivalent of the chronic form of human MGK. It is unknown whether the 11% of animals that exhibited a persistent keratitis without developing secondary keratopathies would do so beyond 8 weeks.

Overview of Pathogenesis and Early Identification of Corneas That Will Not Develop MGK

In rabbit corneas undergoing delayed MGK, injury progression can roughly be divided into 3 stages: (1) the acute injury, which is partially resolved within 1 week; (2) a persistent keratitis characterized by persistent inflammatory sequelae; and (3) development of delayed keratopathies 3 to 5 weeks after exposure. Acute SM toxicity results in cell death and sloughing of the CE through the lamina lucida of the BMZ. Disruption of the epithelial barrier and proinflammatory signaling due to necrosing corneal tissues then lead to corneal edema. Corneas subsequently develop a progressive inflammatory injury between 3 and 5 weeks, with a frequency that is dose dependent. This delayed injury is characterized by RCEs, inflammatory cell infiltrates, bullae, and elevated corneal edema, with associated degradation of the stromal architecture and the BMZ. Notably, significant decreases in corneal edema by 2 weeks after exposure are predictive of injury resolution, suggesting that the underlying pathology of the late SM lesions is present early in the injury process. Kadar et al[17] also reported the early ability to identify resolving corneas based on corneal thickness after goggle-based vapor delivery to the orbital tissues.

The observation that corneas developing MGK did not improve within 8 weeks suggests that either MGK is irreversible at this dose or animals were euthanized before improvement could be detected. The former supposition is supported by electron micrographs of 8-week MGK corneas, which exhibit progressive corneal degeneration, including extensive disruption of the basement membrane, severe stromal distortion, and corneal edema. The clinical status of the small percentage of animals that exhibited a persistent keratitis but did not develop MGK within 8 weeks is unclear. Assuming that persistent keratitis is causally linked to development of the late-onset keratopathies, it seems probable that these animals will ultimately develop MGK. Similarly, even though resolved corneas appear significantly improved compared with MGK corneas, we do not know how these corneas would behave beyond 8 weeks. It may be that some ultimately develop MGK, belying the apparent improvement. If so, this pathology might be equivalent to the delayed-onset injury observed in human casualties, in which an asymptomatic period precedes the appearance of MGK sequelae.

Ultrastructural Data Suggest That Persistent Edema Results in Delayed-Onset Keratopathies

The delayed appearance and increased severity of the delayed injury in cornea provide clues to the specific etiology of MGK. The observations that (1) persistent edema is present in all unresolved animals, (2) changes in edema at 2 weeks are predictive of injury resolution, and (3) many of the secondary keratopathies are associated with persistent edema suggest that edema is the principal pathology of the late SM injury. Corneal edema results from fluid accumulation in the cornea and derives from corneal inflammation or disruption of the corneal epithelial or endothelial barrier. Complications of persistent edema may be symptomatically evidenced through multiple sequelae. For example, unresolved edema within the BLL is likely to hamper successful remodeling of the basement membrane, resulting in persistent cellular necrosis, inflammation, and further degeneration of the anterior segment. A stable and functional basal epithelial cell layer is unlikely to develop because there is no structural scaffold on which to deposit or assemble a functional basement membrane. This is consistent with ultrastructural findings demonstrating severe BMZ disorganization and rarification of the BLL. The inability of basal CE cells to establish permanent adhesions is likely to be destabilizing, leading to the increased deposition of redundant basement membrane components, edema, and CE cell death, resulting in a cyclical phenomenon of sloughing, edema, and failed attempts to reepithelialize.

Whether endothelial cell disruption contributes to persistent corneal edema is currently unknown. Although

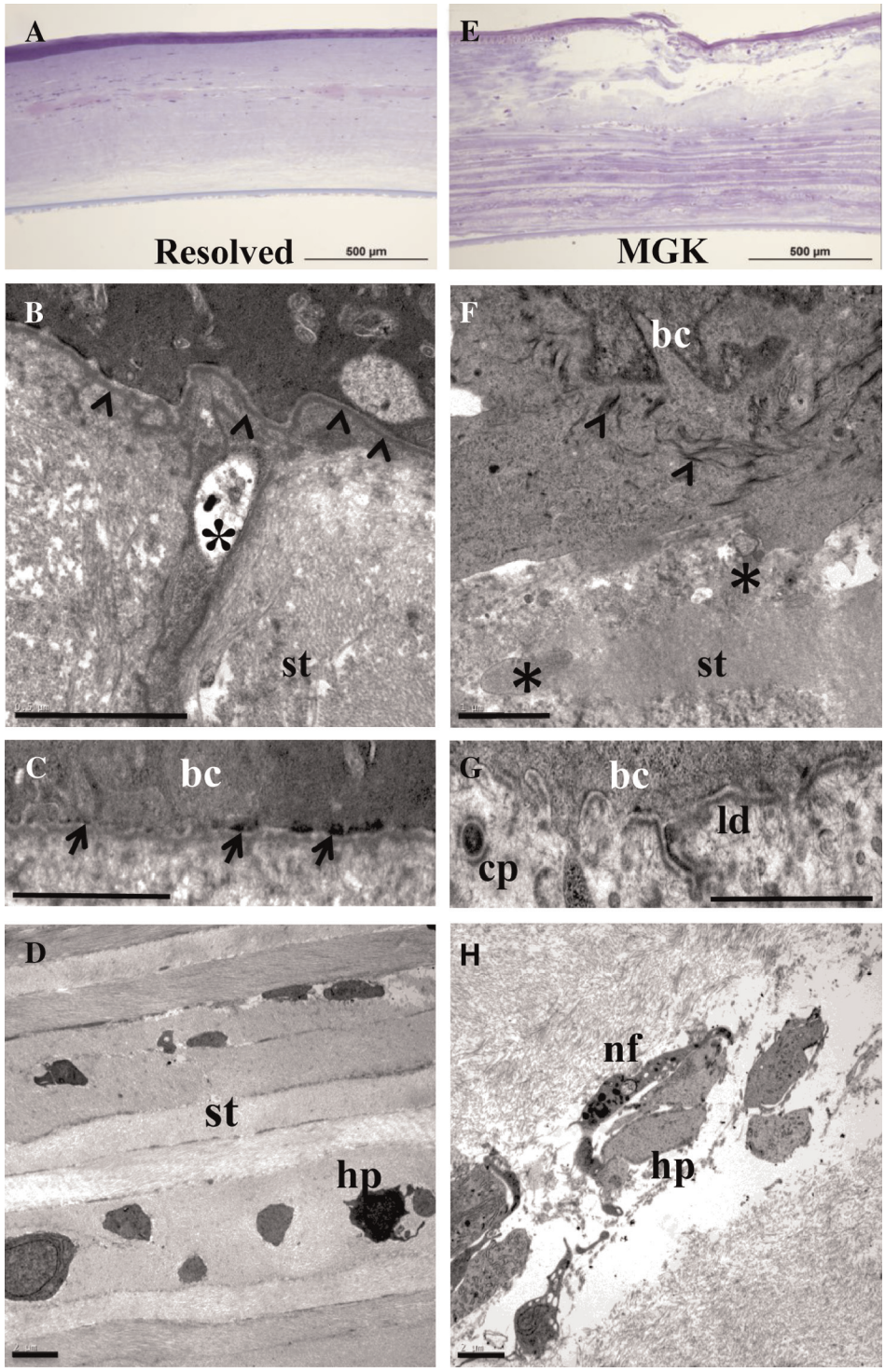

FIGURE 6. Histological and ultrastructural differences between resolved corneas versus those undergoing delayed SM toxicity at 8 weeks. A, Thin section of a resolved cornea. B–D, Electron micrographs of resolved cornea with emphasis of the: (B) BMZ, (C) higher magnification view of BMZ, and (D) stroma. E, Thin section of a MGK cornea. F–H, Electron micrographs of MGK cornea with emphasis of the: (F) BMZ, (G) higher magnification view of BMZ, and (H) stroma. Asterisk indicates representative examples of necrotic remnants, and viable projections (cp) of basal CE cells into the stroma are marked. Arrows indicate basement membrane, and arrowheads indicate hemidesmosomal plaques. bc, basal cell; hp, infiltrating heterophils; ld, lamina densa; nf, necrotic fibrocyte; and st, stroma. Scale bars = 2 μm.

damage to the corneal endothelium would contribute to a loss of barrier function and fluid maintenance within the stroma, there has been no evaluation of endothelial cell toxicity during the acute or delayed SM injury in animal models. In vivo confocal microscopy of human survivors suggests that MGK involves profound decreases in keratocyte and corneal endothelial cell density, providing a mechanism for corneal endothelial barrier dysfunction.[7] The reduction of corneal edema after reepithelialization of the acute lesion between 5 and 14 days indicates some active level of osmotic regulation. However, both delayed corneal endothelial toxicity (eg, due to apoptosis) and RCEs that allow the sustained penetration of protein-rich tear fluid into the stroma could overwhelm the capacity of endothelial cells to deturgesce the stroma.

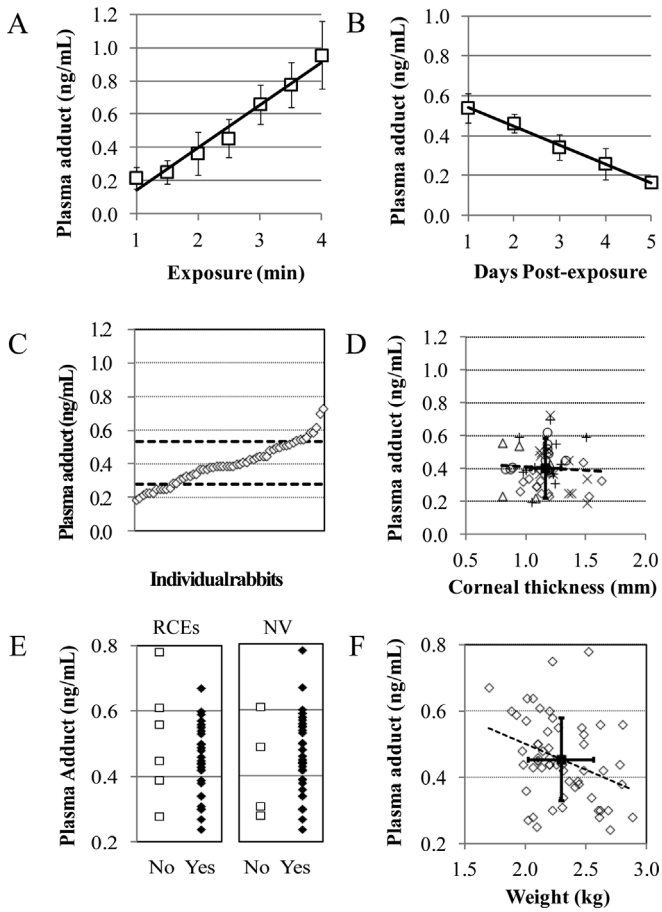

FIGURE 7. Detection, pharmacokinetics, and clinical correlation of plasma protein–SM adducts resulting from ocular vapor SM exposure. A, Dose response showing concentration of plasma adducts 24 hours after 1- to 4-minute ocular exposure to SM vapor (n = 8 per dose). B, Pharmacokinetics of plasma adduct retention after a 2.5-minute exposure (n = 8 per time point). C, Ranked order plasma adduct concentrations (n = 56). Dashed lines are ±1 SD. D–F, Comparison of 1 day plasma adduct concentrations (n = 56) to: (D) 1 week corneal thicknesses (each symbol is a exposure cohort), (E) RCEs at 4 weeks (left) or NV at 6 weeks (right), and (F) Animal weights at time of exposure. Dashed lines represent linear trendline. Solid crosses represent average values ± 1 SD.

Implications of Plasma Adduct Measurements to Toxicological and Therapeutic Evaluations

The ability to quantify SM-adducted proteins in the plasma validated the consistency of ocular exposures. Although the specific routes by which SM and/or adducted protein are absorbed into the vascular system are not clear, radiolabeled SM vapor has been shown to penetrate through the cornea to the lens within 5 minutes.[23,29] The observed disjunction between plasma adduct levels and metrics of acute and delayed injury suggests that individual rabbits exhibit an inherent variability to SM injury, similar to observations from human clinical reports and animal models.[5,17] The mechanism underlying this variability is of interest and may provide a novel therapeutic approach. Conversely, the inclusion of clinically resistant animals in therapeutic trials can complicate therapeutic evaluation, particularly for therapies applied during the first 2 weeks after exposure (ie, before resolving corneas can be identified).

Therapeutic Considerations

Treatment of SM keratopathies is predominantly symptomatic, aimed at managing ocular irritation and improving vision. Due to the broad degenerative nature of delayed-onset sequelae and persistent keratitis, it seems a priori that the optimal therapeutic approach would be to intervene early in the injury process. In animal models, topical corticosteroids, nonsteroidal antiinflammatory agents, and a matrix metalloprotease inhibitor have been therapeutically evaluated within hours to weeks of SM exposure.[16,17] In all cases, these treatments resulted in the transient depression of corneal injury, which subsequently rebounded to levels statistically indistinguishable from exposed controls after cessation of therapy. An alternative delivery mechanism that avoids cyclic dosing may provide a stable therapeutic improvement, but current data suggest that reducing edema or decreasing NV without treating the causative pathology does not prevent long-term corneal keratopathies.[9,17,18]

The eye is a complex structure, with multiple tissues interacting to maintain ocular health. Although no direct SM injury was observed in orbital adnexa using the vapor cup model, it is likely that under typical battlefield conditions, both corneal and noncorneal ocular tissues will suffer direct SM toxicity.[20] In such a scenario, the nature and extent of MGK sequelae may be secondary to injury processes in other tissues. For example, it has been reported that goggle-based SM vapor exposure alters limbal stem cell viability, providing a potential contributory mechanism for RCEs that may not be observed in the corneal vapor exposure model.[17] Thus, to expand the range of therapeutic targets, we are currently exploring how the interaction between corneal and noncorneal injury processes influences MGK development.

The temporal gap observed between the acute injury and clinical detection of delayed corneal keratopathies may imply a secondary etiology. Potential mechanisms include injuries to supportive tissues or destructive modifications to extracellular material. For example, cells responsible for corneal remodeling may encounter chemically adducted proteins and subsequently initiate a proinflammatory cascade.[27] Alternatively, chemical modification may interfere with the ability of CE cells to stably attach. It is possible that intoxication of limbal or corneal cell populations may have a delayed effect on cell viability, such as inducing apoptosis through disruption of DNA synthesis or RNA transcription.[30–32] Although alkylation of protein and nuclear material can influence cell fate, the direct consequences of adduct formation on acute and long-term corneal sequelae have not yet been addressed.

These data demonstrate a system-based approach combining ultrastructural analysis, histochemistry, and molecular evaluation that links architectural changes in

corneal structure with clinical outcomes and posits potential mechanisms for the pathogenesis of SM corneal lesions. The identification of such mechanisms is critical to designing effective therapeutic modalities that prevent the development of acute and delayed lesions and may be applicable to persistent keratopathies unrelated to SM alkylation.

ACKNOWLEDGMENTS

The authors acknowledge the sustained technical support provided by Megan Lyman, Kaylie Tuznik, Kim Whitten, Paula Adkins, Kathy King, Lindsey Devine, and Susan Schulz (United States Army Medical Research Institute of Chemical Defense); the advice and support of Dr. Gabe Sosne (Wayne State University); and Dr. Jeffrey Yourick and the Defense Threat Reduction Agency for encouragement and financial support.

REFERENCES

1. Papirmeister B, Feister AJ, Robinson SI, et al. *Medical Defense Against Mustard Gas: Toxic Mechanisms and Pharmacological Implications*. Boca Raton, FL: CRC Press; 1991.
2. Javadi MA, Yazdani S, Kanavi MR, et al. Long-term outcomes of penetrating keratoplasty in chronic and delayed mustard gas keratitis. *Cornea*. 2007;26:1074–1078.
3. Mousavi B, Soroush MR, Montazeri A. Quality of life in chemical warfare survivors with ophthalmologic injuries: the first results form Iran Chemical Warfare Victims Health Assessment Study. *Health Qual Life Outcomes*. 2009;7:2.
4. Khateri S, Ghanei M, Keshavarz S, et al. Incidence of lung, eye, and skin lesions as late complications in 34,000 Iranians with wartime exposure to mustard agent. *J Occup Environ Med*. 2003;45:1136–1143.
5. Javadi MA, Yazdani S, Sajjadi H, et al. Chronic and delayed-onset mustard gas keratitis: report of 48 patients and review of literature. *Ophthalmology*. 2005;112:617–625.
6. Richter MN, Wachtlin J, Bechrakis NE, et al. Keratoplasty after mustard gas injury: clinical outcome and histology. *Cornea*. 2006;25:467–469.
7. Jafarinasab MR, Zarei-Ghanavati S, Kanavi MR, et al. Confocal microscopy in chronic and delayed mustard gas keratopathy. *Cornea*. 2010;29:889–894.
8. Lagali N, Fagerholm P. Delayed mustard gas keratitis: clinical course and in vivo confocal microscopy findings. *Cornea*. 2009;28:458–462.
9. Babin M, Ricketts KM, Gazaway M, et al. A combination treatment for ocular sulfur mustard injury in the rabbit model. *Cutan Ocul Toxicol*. 2004;23:65–75.
10. Anumolu SS, DeSantis AS, Menjoge AR, et al. Doxycycline loaded poly (ethylene glycol) hydrogels for healing vesicant-induced ocular wounds. *Biomaterials*. 2010;31:964–974.
11. Solberg Y, Alcalay M, Belkin M. Ocular injury by mustard gas. *Surv Ophthalmol*. 1997;41:461–466.
12. Mann I, Pullinger BD. A study of mustard gas lesions of the eyes of rabbits and men (Section of Ophthalmology). *Proc R Soc Med*. 1942;35:229–244.
13. Petrali JP, Dick EJ, Brozetti JJ, et al. Acute ocular effects of mustard gas: ultrastructural pathology and immunohistopathology of exposed rabbit cornea. *J Appl Toxicol*. 2000;20(suppl 1):S173–S175.
14. Marzulli FN, Maibach HI. *Dermatotoxicology*. Washington, DC: Taylor & Francis; 1996.
15. Gates M, Moore S. *Mustard Gas and Other Sulphur Mustards*. Washington, DC: Office of Scientific Research And Development; 1946:30–58.
16. Amir A, Turetz J, Chapman S, et al. Beneficial effects of topical anti--inflammatory drugs against sulfur mustard-induced ocular lesions in rabbits. *J Appl Toxicol*. 2000;20(suppl 1):S109–S114.
17. Kadar T, Dachir S, Cohen L, et al. Ocular injuries following sulfur mustard exposure—pathological mechanism and potential therapy. *Toxicology*. 2009;263:59–69.
18. Gordon MK, Desantis A, Deshmukh M, et al. Doxycycline hydrogels as a potential therapy for ocular vesicant injury. *J Ocul Pharmacol Ther*. 2010;26:407–419.
19. Kadar T, Turetz J, Fishbine E, et al. Characterization of acute and delayed ocular lesions induced by sulfur mustard in rabbits. *Curr Eye Res*. 2001;22:42–53.
20. Milhorn D, Hamilton T, Nelson M, et al. Progression of ocular sulfur mustard injury: development of a model system. *Ann N Y Acad Sci*. 2010;1194:72–80.
21. Capacio BR, Smith JR, DeLion MT, et al. Monitoring sulfur mustard exposure by gas chromatography-mass spectrometry analysis of thiodiglycol cleaved from blood proteins. *J Anal Toxicol*. 2004;28:306–310.
22. Graham JS, Chilcott RP, Rice P, et al. Wound healing of cutaneous sulfur mustard injuries: strategies for the development of improved therapies. *J Burns Wounds*. 2005;4:e1.
23. Noort D, Fidder A, Degenhardt-Langelaan CE, et al. Retrospective detection of sulfur mustard exposure by mass spectrometric analysis of adducts to albumin and hemoglobin: an in vivo study. *J Anal Toxicol*. 2008;32:25–30.
24. Surovikina MS. The half-life of the different serum protein fractions in the circulating blood. *Bull Exp Biol Med*. 1957;43:172–175.
25. Dixon FJ, Maurer PH, Deichmiller MP. Half-lives of homologous serum albumins in several species. *Proc Soc Exp Biol Med*. 1953;83:287–288.
26. Little RA. Changes in the blood volume of the rabbit with age. *J Physiol*. 1970;208:485–497.
27. Naderi M, Jadidi K, Falahati F, et al. The effect of sulfur mustard and nitrogen mustard on corneal collagen degradation induced by the enzyme collagenase. *Cutan Ocul Toxicol*. 2010;29:234–240.
28. Maumenee AE, Scholz RO. The histopathology of the ocular lesions produced by the sulfur and nitrogen mustard. *Bull Johns Hopkins Hosp*. 1948;82:121–147.
29. Axelrod DJ, Hamilton JG. Radio-autographic studies of the distribution of lewisite and mustard gas in skin and eye tissues. *Am J Pathol*. 1947;23:389–411.
30. Lin P, Vaughan FL, Bernstein IA. Formation of interstrand DNA cross-links by bis-(2-chloroethyl)sulfide (BCES): a possible cytotoxic mechanism in rat keratinocytes. *Biochem Biophys Res Commun*. 1996;218:556–561.
31. Lin PP, Bernstein IA, Vaughan FL. Bis(2-chloroethyl)sulfide (BCES) disturbs the progression of rat keratinocytes through the cell cycle. *Toxicol Lett*. 1996;84:23–32.
32. Masta A, Gray PJ, Phillips DR. Effect of sulphur mustard on the initiation and elongation of transcription. *Carcinogenesis*. 1996;17:525–532.